Original Article

Institution of MECHANICAL ENGINEERS
Journal of ENGINEERING IN MEDICINE

Proc IMechE Part H:
J Engineering in Medicine
2022, Vol. 236(4) 583–591

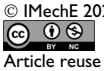
Article reuse guidelines:
sagepub.com/journals-permissions
DOI: 10.1177/09544119221075400
journals.sagepub.com/home/pih


Towards catheter steering using magnetic tractor beam coupling

Chayabhan Limpabandhu[1], Yihua Hu[1], Hongliang Ren[2], Wenzhan Song[3] and Zion Tse[1]

Abstract

Catheters are used in various clinical applications, and the ability to direct the catheter to the desired location is critical for clinical outcomes. Steerable catheters assist clinicians to access targeted areas, notably the vascular bundles and major vessels, while causing no damage to the surrounding tissue. A novel catheter actuation technology for catheter steering is presented in this study. The technique is simple and relies on three magnetic couples interacting with one another to generate steering motions. A proof-of-concept catheter prototype demonstrated the capacity to remotely steer a catheter over 100 mm of distance and $\pm 45°$ of angular positioning, showing the potential manoeuvrability for clinical applications. It is feasible to steer a catheter using this three-magnet pair approach with the great potential to be used for catheterisation procedures. The presented mechanism's kinematics and a near-form solution for catheter steering regardless of design factors will be studied in the future.

Keywords

Magnetic actuation, magnetic actuation catheter, magnetic navigation, magnetic navigation catheter, steerable catheter

Date received: 17 August 2021; accepted: 21 December 2021

Introduction

According to the World Health Organization, 19.3 million new cancer cases were discovered, and 10 million cancer deaths occurred worldwide last year.[1] Lung cancer is the second leading cause of cancer death and the second most prevalent cancer in the world. Early detection and diagnosis and accurate localisation in lung intervention are essential to reducing lung cancer fatalities.[2,3]

Bronchoscopic treatments have been used to treat lung cancer for decades, including methods such as ablative technology in which a catheter uses an energy source to burn cancerous tissue.[4,5] Despite their long history, ablative technologies are still being developed today. Some recent examples are a three-dimensional (3D) kinematic steerable ablation catheter in which the catheter is actuated by magnetic forces generated by the magnetic field of magnetic resonance imaging (MRI), a bendable catheter used for bronchoscopic radiofrequency ablation (RFA), and the use of real-time MRI technologies to navigate custom-designed catheters.[6–8]

Catheters are used in various clinical applications,[9–11] and the ability to guide catheters to desired locations is critical to cancer treatment success.[12–15] Nonetheless, catheter guidance still has significant limitations, particularly for deep-seated tumours where the catheter must be inserted deep into the body. Additionally, catheter steering becomes much more difficult when nearby tissues are delicate and might be punctured if clinicians push overly forcefully.

Precision in manual catheter navigation and placement is complex and requires considerable training for the surgeon. For this issue, robotic navigation and steering are possible solutions that can be integrated with current equipment and processes.

An easily steerable catheter would allow clinicians to reach target organs accurately[16] and effectively avoid damage to surrounding tissue.[17] Many researchers have developed various catheters. For example, a unique

[1]Department of Electronic Engineering, University of York, York, UK
[2]Department of Electronic Engineering, The Chinese University of Hong Kong, Hong Kong
[3]School of Electrical and Computer Engineering, University of Georgia, GA, USA

Corresponding author:
Zion Tse, Department of Electronic Engineering, University of York, YO10 5DD Heslington, York, England.
Email: zion.tse@york.ac.uk

multi-steerable catheter with four degrees of freedom was designed, resulting in increased steerability.[18] An external magnetic field was also applied to actuate a catheter capable of steering and unclogging actions, which increased its therapeutic mobility and functioning in blood vessels.[19] MRI was also used to guide a catheter using magnetic gradients to maximise deflections.[20]

Magnetic fields are used to actuate and guide catheters in many clinical applications using an electromagnetic coil and permanent magnets. As an example, the external force from electromagnetic systems is used to guide and actuate the magnetic drilling catheter, which is remotely guided with high torques towards curved paths, and the catheter can be fully inserted into the body to achieve access to all abdominal quadrants.[21,22] In addition, a permanent magnet is used to actuate and manipulate a five-degrees-of-freedom wired robot to perform laparoendoscopic single-site surgery. It is also used to produce the same degree of control over unconstrained microscale devices to increase magnetic field and gradient strength.[23,24]

The conventional method of catheter steering relies on the operator controlling the catheter at the proximal end and has a limited range of steering motion and flexibility. As a catheter is a long, flexible tube, manoeuvring a catheter relies heavily on the experience and visual-motor coordination of the operator. Furthermore, the accuracy and safety of catheter steering are influenced by the complexity of the route and target location. Reduced force feedback from the catheter tip to the catheter handle could lead to tissue perforation since the operator may push the catheter too hard. In cardiac procedures, perforation with resulting tamponade is a major complication. Therefore, a new method for catheter steering is presented in this paper based on the principle of directly moving the catheter tip as opposed to controlling the catheter tip remotely through the catheter handle. This method could potentially increase the motion and flexibility capabilities of catheters and avoid excessive force during catheter steering.

This paper presents a new catheter actuation approach inspired by the tractor beam, a fictitious device used to move items remotely, such as in the Star Wars films. Our idea is based on three magnetic couples interacting with each other to generate two-dimensional motions. Tests of the proposed actuation approach indicate that it can guide a catheter with the needed manoeuvrability for a variety of clinical applications.

Mathematical magnetic equations

The symbols of notation can be found in Table 1.

Table 1. Symbols of notation.

Symbol	Description
ℓ_e	Effective length
O	Origin of magnet
N	North pole
S	South pole
L	Length from origin to one of the poles
Φ_B	Magnetic flux
B	Magnetic field
A	Surface area
μ	Magnetic moment / Magnetic dipole moment
Br_{max}	Maximum residual flux density
V	Volume of the magnet
μ_0	Permeability of a vacuum

The effective length of a magnet

Permanent magnets typically create powerful and long-lasting magnetic fields. A magnet's shape and size determine the strength and dispersion of its magnetic field. According to Figure 1(a), the magnetic length (ℓ_e) is defined as the distance between two of the magnetic poles in which the centre of the magnet is the origin (O). According to Figure 1(a):

$$\ell_e = ON = OS = L$$

Magnetic flux (Φ_B)

Magnetic flux is often called the 'lines of force' (Figure 1(b)), which have a definite direction from the North to the South pole, never cross each other, and are continuous. It is a static region around a magnet in which the magnetic force exists, and the magnetic field is strongest near the pole of a magnet since the lines of force are closer together. The magnetic flux can be calculated as:

$$\Phi_B = \iint_A B \cdot dA$$

Magnetic field (B)

The number of lines of force within a given unit area is referred to as the magnetic field or magnetic flux density. It expresses the intensity of a magnetic field at a specific region in force per unit length. It can be calculated as:

$$B = \frac{\Phi_B}{A}$$

The two poles of a magnet behave differently. The attraction of two magnets is more robust than their repulsion due to the magnet's molecular magnets

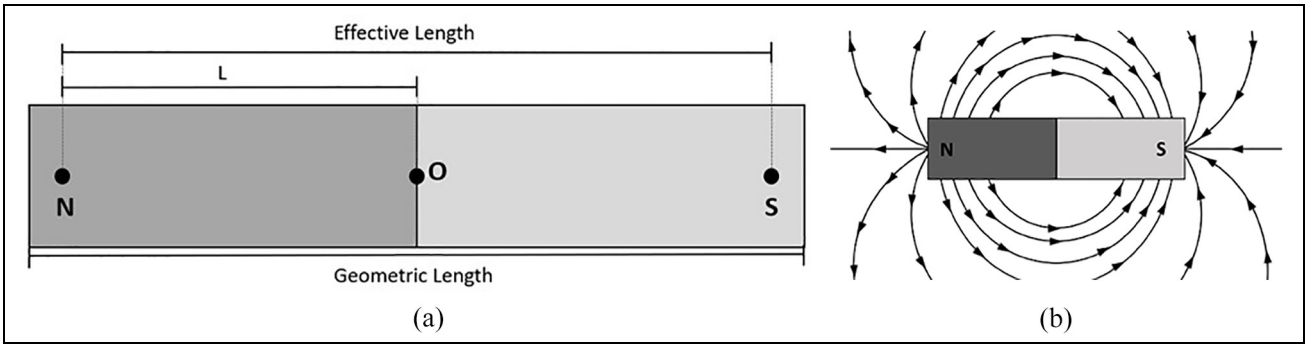

Figure 1. Magnet principle of a bar magnet: (a) magnet's effective and geometric length and (b) magnetic field line of flux.

becoming aligned when two different magnetic poles attract each other; one magnet promotes the parallel alignment of the molecular magnets in the other magnet. In contrast, when two equal magnetic poles repel one other, both magnets are weakened, as one magnet interrupts the parallel alignment of the molecular magnets of the other magnet.

Magnetic moments and dipoles

The magnetic moment (μ), also known as the magnetic dipole moment, is a vector that quantifies the torque encountered by a particular magnet in an external magnetic field. This magnetic property is frequently depicted as radiating from the north and south poles. The magnetic dipole moment can be calculated by:

$$\boldsymbol{\mu} = \mathbf{Br}_{max} \times \frac{V}{\boldsymbol{\mu}_0}$$

where Br_{max} indicates the maximum flux output from the magnetic material and is the point at which the hysteresis loop crosses the B axis at zero magnetising force and

$$\boldsymbol{\mu}_0 = 4\pi \times 10^{-7}\ {}^{N}/_{A^2}$$

Method and procedures

List of magnets used and their properties

This paper uses nine magnets categorised into three experiments with three positions: Lead magnet, Co-lead magnet and Follower magnet. A list of magnets and their properties are provided in Table 2.

Idea verification experiment

A tractor beam magnet, also known as an inverter magnet, consists of a set of magnets. A single magnetic field is produced, and another magnet, known as the follower magnet, is positioned at a specified distance. The follower magnet, as the title implies, follows the movement of the inverter magnet. A simple experiment

Table 2. List of magnets used in the experiment and their properties.

Experiment	Position	Size	Grade	Magnetic flux density (B) (gauss)	Magnetic dipole moment (μ) (Am^2)
Idea Verification Experiment	Lead	25 *mm diameter*×5 *mm thickness*	N42	2451	2.58
	Co-lead	10×5×4 *mm*	N42	4807	0.210
	Follower	14 *mm diameter*×4 *mm thickness*	N42	3274	0.647
COMSOL Concept Simulation	Lead	20 *mm diameter*×10 *mm thickness*	N52	5233	3.70
	Co-lead and Follower	6 *mm diameter*×10 *mm thickness*	N52	7088	0.333
Proof of Concept Experiment	Lead	25 *mm diameter*×10 *mm thickness*	N42	4123	5.16
	Co-lead	10×5×10 *mm*	N42	6143	0.525
	Follower	3 *mm diameter*×6 *mm thickness*	N42	6403	0.0445
Magnetic Tractor Beam's Distance Experiment	Lead	20 *mm diameter*×10 *mm thickness*	N52	5233	3.70
	Lead	17 *mm diameter*×10 *mm thickness*	N52	5638	2.67
	Co-lead and Follower	8 *mm diameter*×10 *mm thickness*	N52	6871	0.592
	Co-lead and Follower	6 *mm diameter*×10 *mm thickness*	N52	7088	0.333
Catheter Model	Lead	50×50×25 *mm*	N52	4933	73.6
	Co-lead	40×20×20 *mm*	N52	7190	1.88
	Follower	5 *mm diameter*×20 *mm thickness*	N42	6549	0.413

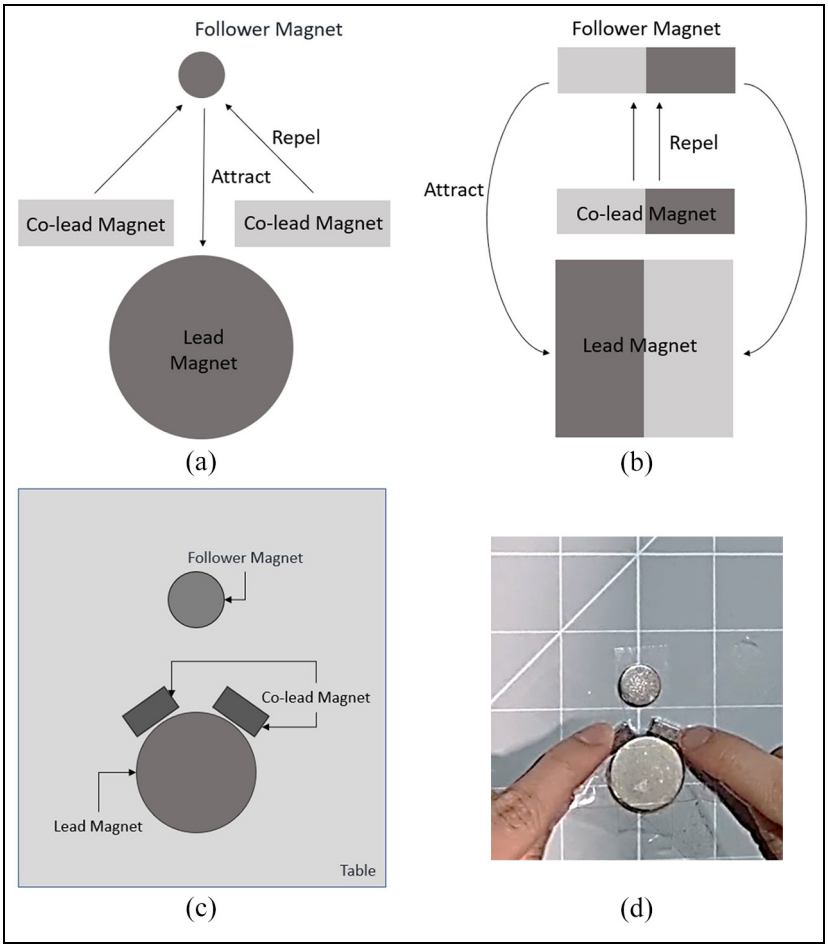

Figure 2. Magnet diagram of the magnetic inverter: (a) front view of inverter magnet concept, (b) side view of inverter magnet concept, (c) diagram of the idea verification experiment and (d) idea verification experiment setup.

was carried out to test this phenomenon. To begin, an inverter magnet and another magnet (the follower magnet) were set on opposing sides of a table. Then, the inverter magnet was moved closer to the follower magnet until it began to move. Typically, depending on their orientation, two magnets would resist or collide. The inverter magnet and follower magnet, on the other hand, maintained a constant distance. Even though the magnets only interacted through magnetic forces, when the inverter magnet was moved over the table's surface, the follower magnet followed as if they were attached to each other with a hard chain.

Based on the current design of the inverter magnet, which employs a cylindrical magnet, a catheter actuation principle was developed. Moving the co-lead magnets closer together causes the follower magnet to travel farther away from the inverter magnet, and moving the co-lead magnets farther apart causes the follower magnet to move closer to the inverter magnet. It is assumed that with this setup (Figure 2), the user will be able to regulate the distance of the follower magnet. Three magnets were placed on a table to demonstrate the concept (Figure 2(c)). The lead magnet was taped to the table, and the two co-lead magnets were moved by hand to see whether the magnetic couples could manipulate the follower magnet or not.

COMSOL concept simulation

A magnetic simulation was constructed in COMSOL (Stockholm, Sweden) to understand the concept's relationship between magnets. By setting up a 'Magnetic Fields, No Currents (mfnc)' with the 'Stationary' studies, a set of magnets made from the 'N52 (Sintered NdFeB)' magnet material was modelled in COMSOL to see their magnetic flux density and force diagram. The magnets' material properties can be seen in Table 3. The result simulation studies are created in a 3D plane, and a 2D plane is cut in the middle of all the magnets to determine the magnetic density.

Proof of concept experiment

In order to prove that the follower magnet is able to be manipulated in the y-axis by our set of magnets, an initial simple prototype was developed and built. An acrylic sheet, chopstick, shielding sheet, and magnets made up the prototype. First, the acrylic sheet was cut

Table 3. Material properties of magnets used in the simulation.

Property	Expression
Relative permittivity	1
Recoil permeability	1.05
Thermal conductivity	9 $Wm^{-1}K^{-1}$
Density	7.55 gcm^{-3}
Heat capacity at constant	440 $Jkg^{-1}K^{-1}$
Electrical conductivity	1/1.5 $u\Omega \cdot m$
Relative permittivity	1
Remanent flux density norm	1.44 T

into pieces, and a glue gun was used to adhere them to the magnet. The shielding sheet was then attached to two acrylic sheets connected to the co-lead magnets to minimise the magnetic strength when moving the magnets by hand. To mock a catheter during surgery, the follower magnet was connected to the tip of the chopstick. The follower magnet was examined to see if it could move up and down the Y plane.

Magnetic tractor beam (MTB) experiment

Magnetics with different sizes and field strengths were tested out for the MTB effect. The distances between two co-lead magnets were studied again as well as the distances between the leading magnet and the following magnet to understand the range of the MTB effect. After that, different magnet holes and combinations of pegboards were modelled according to the minimum and maximum distance measured in SOLIDWORKS and cut by the laser cutter machine (Figure 3). The magnets were inserted into each hole, and the distance between the lead magnet and follower magnet was measured. The measurement was repeated until all possible distances were measured. Moreover, to see whether different arrangements of magnets could hold the magnet in the air vertically upside down or not, the pegboard was placed vertically. If the follower magnet could levitate in the air, the distance between the lead magnet and follower magnet was measured once again. After that, to see whether the weight of the follower magnet affected the distance between the lead magnet and follower magnet, grains of long-grain white rice were added to the follower magnet and the distance was measured once more. In this experiment, three grains of rice (each 25 mg) were added one by one. All distances were measured. Every measurement was repeated three times, and the mean was calculated as a result.

Catheter model

The second prototype, pictured in Figure 4, was designed in SOLIDWORKS. The objective for this prototype was to move the follower magnet in the XY plane. The follower magnet was moved in the X plane manually, whereas it was moved in the Y plane by moving the Co-lead magnets. As the magnet strength

Figure 3. Example of pegboard. Printed 3D model with magnets inserted into the pegboard.

was powerful, seven small blocks ($6\times6\times70$ *mm*) were designed to distinguish the Co-lead magnets to identify each distance. A 3D printer was used to create each element of the model, and then the elements were assembled with the magnets. A small magnet was placed inside a 5 mm catheter above the prototype. Finally, the distance enabling the tractor beam effect and the distance between the lead magnet and the follower magnet were measured.

Result and discussion

COMSOL simulation

Displaying the results of the COMSOL simulation, Figure 5 shows that the lead magnet and follower magnet attract each other, whereas the co-lead magnets repel the follower magnet. These opposing forces are responsible for creating a gap between the follower magnet and the lead/co-lead magnets.

Magnetic tractor beam distance

The MTB distance was subject to the size of the magnet (Figure 6). The distance between the lead magnet and follower magnet was first measured horizontally, and the result is shown in Figure 7(a). However, only two combinations of magnets could hold the follower magnet upside down. The distance between the lead and follower magnet was measured for these two combinations, and the results are shown in Figure 7(b). The distance that could hold the follower magnet most stably was the maximum distance between the co-lead magnets.

Figure 7 shows the curve fitting results of the experiment. The distance between the lead magnet and follower magnet is inversely proportional to the distance between the two co-lead magnets. Additionally, with the pegboard placed horizontally, when the follower

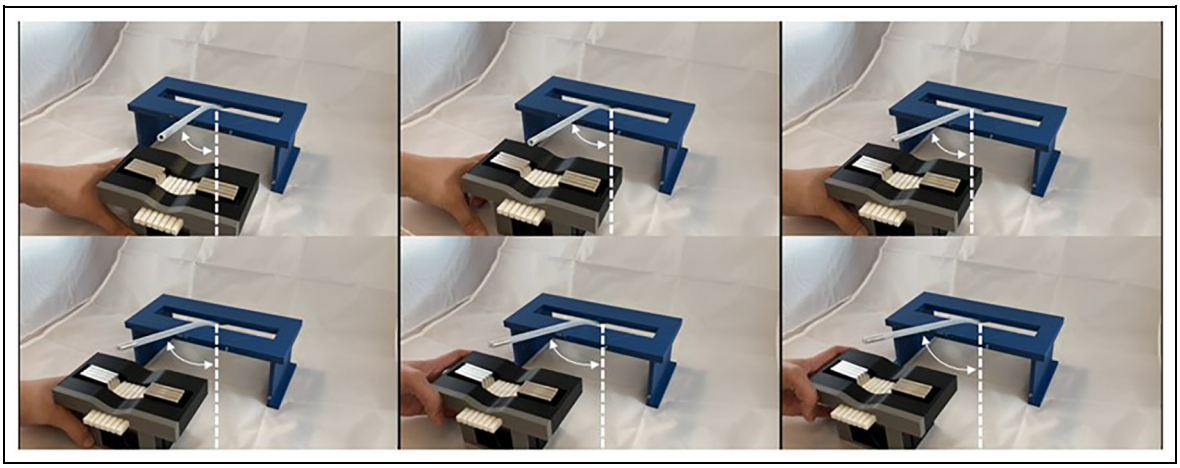

Figure 4. 3D printed catheter model experiment. The catheter is held by the magnets and is moved from position A to F by the co-lead magnets. White arrows and lines denote the range of motion from 0° to 45°, where the solid line is the initial position (0°), and the dashed line is the catheter position.

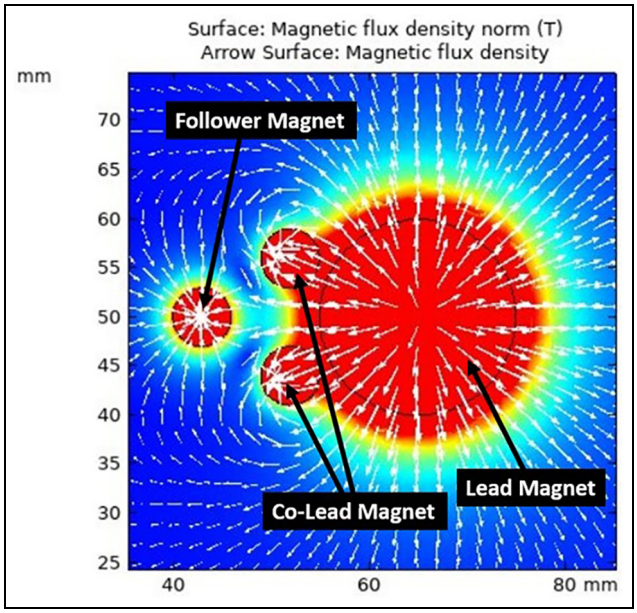

Figure 5. COMSOL simulation of MTB plane cut's magnetic flux density norm. The arrows show the magnetic flux directions between the four magnets.

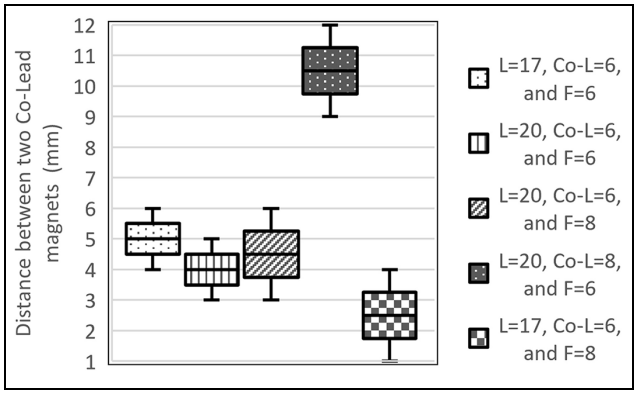

Figure 6. Distance between two Co-lead magnets that enable the tractor beam effect, where L = Lead magnet, Co-L = Co-lead magnets, and F = Follower magnet, and the values of L, Co-L, and F are the diameter of the magnets in mm. All of the magnets are in grade N52.

magnet is bigger than the co-lead magnet, the distance between the lead and follower magnet is smaller than when the co-lead magnet and follower magnet are the exact sizes. Furthermore, when the lead magnet is 17 mm long, the distance between the lead magnet and follower magnet is bigger than when the lead magnet is 20 mm long. However, when the lead magnet is either 17 or 20 mm long and the distance between co-lead magnets is the minimum, the follower magnet cannot be held vertically upside down, as the magnetic flux of the co-lead magnets is overpowered by that of the lead magnet. Moreover, as the systems have been placed upside down, there was a gravitational force acting on the follower magnet, resulting in the weight of the follower magnet affecting the distance between the lead and follower magnets; as the distance increases when it is measured vertically upside-down (Figure 7(c)).

Catheter model experiment

The two co-lead magnets were moved closer to and farther away from each other during the experiment with the catheter model. Figure 8 shows that the MTB effect is only possible for a certain range of distances between the co-lead magnets; in this case, the distance between co-lead magnets ranged from 6 to 36 mm. The catheter model with an inserted following model demonstrated the capacity to steer over 75–103 mm of distance (in the vertical plane) and ±45 degrees of angular positioning (in the horizontal plane), showing the potential manoeuvrability for clinical applications

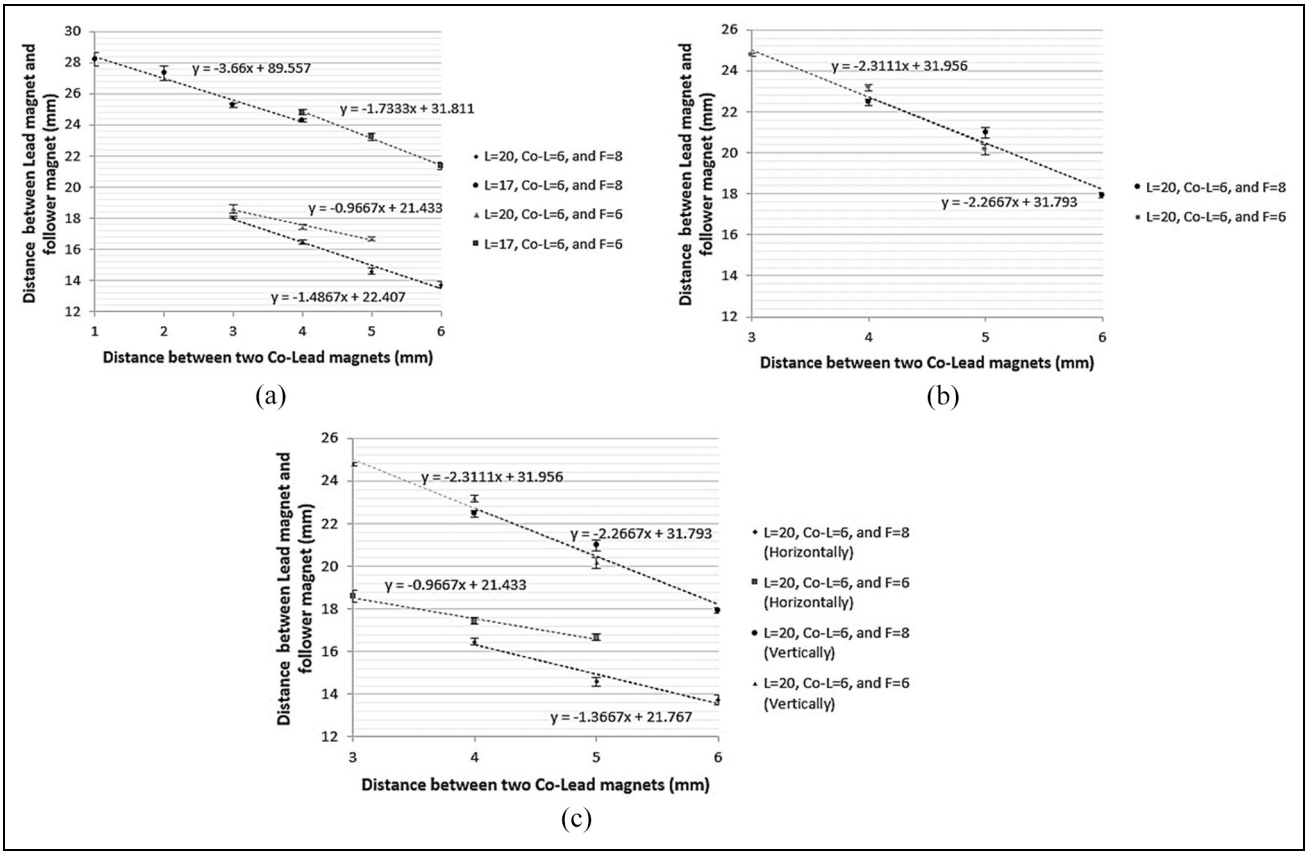

Figure 7. Distance between the lead magnet and follower magnet, where L = Lead magnet, Co-L = Co-lead magnets, and F = Follower magnet, and the values of L, Co-L, and F are the diameters of the magnets in mm. The standard deviation is plotted in the graph as an error bar. (a) pegboard placed horizontally, (b) pegboard placed vertically upside-down and (c) comparing distance results when the pegboard is placed horizontally and vertically.

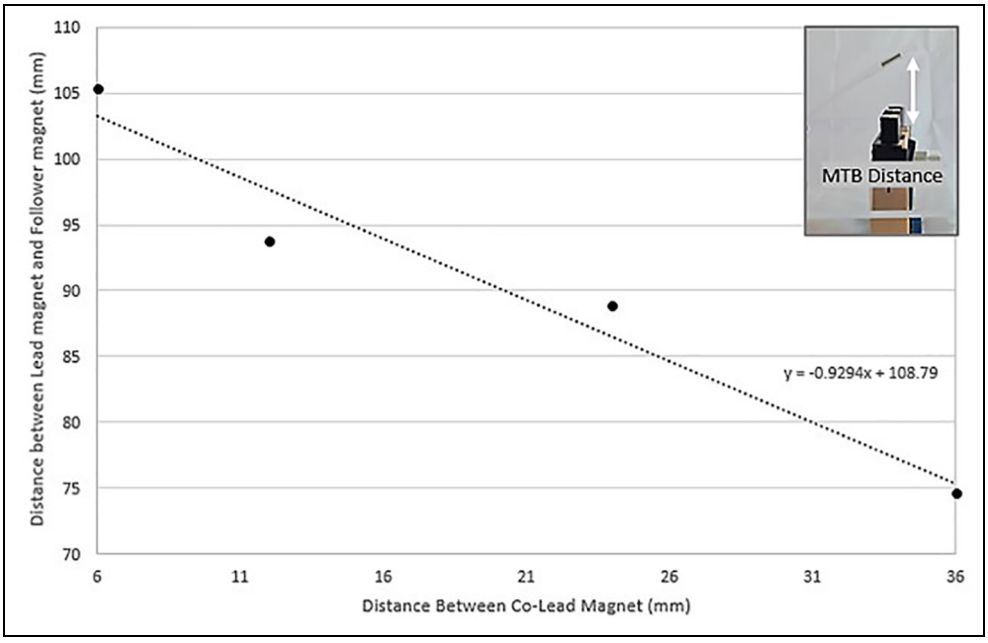

Figure 8. Distances between Co-lead magnets that enable MTB and MTB distances (distance between the lead magnet and follower magnet) in the catheter model.

The catheter can be manipulated in both vertical and horizontal planes by the three-magnet pair approach even if only certain distances enable the tractor beam effect. Although the co-lead magnets control the distance between the lead and follower magnet, the lead magnet still has a lead role in manipulating the magnet, as it is the magnet that attracts the follower magnet. When the magnetic field lines of the co-lead magnets cancel out all of the magnetic field lines of the lead magnet, this breaks the tractor beam effect. If the co-lead magnets are too far from each other, there will be no repulsion between the co-lead magnet and the follower magnet, and the tractor beam effect will not occur.

Traditional catheters have limited steering capabilities, which is particularly problematic for deep-seated tumours requiring the catheter to be inserted deep into the body. Clinicians can easily apply too much force and accidentally puncture tissue, especially when the surrounding tissues are delicate. The presented method will significantly improve catheter steering by allowing clinicians to wirelessly steer the catheter from the tip in the horizontal and vertical planes.

Conclusion and future works

This study illustrates the MTB magnet's potential for use in various purposes in medical applications. According to our concept verification, a catheter inserted with a follower magnet can be manipulated spatially. The result shows that only specific distances enable MTB, and some combinations of magnets are not able to hold the follower magnet upside down. Different sizes and combinations of magnets result in different steering distances.

Mathematical modelling of the MTB effect in 3D is recommended to study with how MTB magnets influence each other. Also, setting up a proof of concept model for catheter steering and a model required for the steering distance required according to the clinical requirement need to be done. Future studies include studies of the MTB effect in more depth, including simulations and experimental studies on the magnetic flux, force and distance of magnets in different sizes and combinations. Follow up by the catheter position's characterisation and force studied, and a study on an anatomical model. Establishing a closed-form kinematic solution for MTB-based steering under various design conditions should be studied involved in an additional study.

Acknowledgement

We thank Mike Angus (Laboratory Technician, Department of Electronic Engineering, University of York) for his guidance and contributions towards the 3D printing of our research.

Author contributions

All authors developed the concept and the design of the work. CL contributed to the acquisition of the experiment under the supervision of ZT. CL revised the work, and all authors approved the final manuscript for publication.

Funding

The author(s) disclosed receipt of the following financial support for the research, authorship, and/or publication of this article: This study was supported in part by the Royal Society Wolfson Fellowship, the National Institutes of Health (NIH) Bench-to-Bedside Award, the NIH Center for Interventional Oncology Grant, the National Science Foundation (NSF) I-Corps Team Grant (1617340), NSF REU site program 1359095, the UGA-AU Inter-Institutional Seed Funding, the American Society for Quality Dr. Richard J. Schlesinger Grant, the PHS Grant UL1TR000454 from the Clinical and Translational Science Award Program, and the NIH National Center for Advancing Translational Sciences, the NIH Center for Interventional Oncology: Grant ZID# BC011242 & CL040015 and supported by the Intramural Research Program of the National Institutes of Health.

ORCID iD

Chayabhan Limpabandhu https://orcid.org/0000-0002-6560-8768

References

1. Sung H, Ferlay J, Siegel RL, et al. Global cancer statistics 2020: GLOBOCAN estimates of incidence and mortality worldwide for 36 cancers in 185 countries. *CA Cancer J Clin* 2021; 71: 209–249.
2. Midthun DE. Early detection of lung cancer. *F1000Res* 2016; 5: 2–7.
3. Sutedja G. New techniques for early detection of lung cancer. *Eur Respir J* 2003; 21: 57s–66s.
4. Chaddha U, Hogarth DK and Murgu S. Bronchoscopic ablative therapies for malignant central airway obstruction and peripheral lung tumors. *Ann Am Thorac Soc* 2019; 16: 1220–1229.
5. Sabath BF and Casal RF. Bronchoscopic ablation of peripheral lung tumors. *J Thorac Dis* 2019; 11: 2628–2638.
6. Xie F, Zheng X, Xiao B, et al. Navigation bronchoscopy-guided radiofrequency ablation for nonsurgical peripheral pulmonary tumors. *Respiration* 2017; 94: 293–298.
7. Heidt T, Reiss S, Krafft AJ, et al. Publisher correction: real-time magnetic resonance imaging – guided coronary intervention in a porcine model. *Sci Rep* 2019; 9: 18282–18310.
8. Liu T, Poirot NL, Franson D, et al. Modeling and validation of the three-dimensional deflection of an MRI-compatible magnetically actuated steerable catheter. *IEEE Trans Biomed Eng* 2016; 63: 2142–2154.

9. Wobith M, Wehle L, Haberzettl D, et al. Needle catheter jejunostomy in patients undergoing surgery for upper gastrointestinal and pancreato-biliary cancer-impact on nutritional and clinical outcome in the early and late postoperative period. *Nutrients* 2020; 12: 2564.
10. Naranjo J, Portner ER, Jakub JW, et al. Ipsilateral intravenous catheter placement in breast cancer surgery patients. *Anesth Analg* 2021; 133: 707–712.
11. Assadsangabi B, Tee MH, Wu S, et al. Catheter-based microrotary motor enabled by ferrofluid for microendoscope applications. *J Microelectromech Syst* 2016; 25: 542–548.
12. Chen Y, Xu S, Squires A, et al. MRI-guided robotically assisted focal laser ablation of the prostate using canine cadavers. *IEEE Trans Biomed Eng* 2018; 65: 1434–1442.
13. Inoue K, Owaki T, Nakamura T, et al. Clinical application of transvenous mitral commissurotomy by a new balloon catheter. *J Thorac Cardiovasc Surg* 1984; 87(3): 394–402.
14. Dotter CT. Catheter biopsy experimental technic for transvenous liver biopsy. *Radiology* 1964; 82: 312–314.
15. Yagihashi K, Takizawa K, Ogawa Y, et al. Clinical application of a new indwelling catheter with a side-hole and spirally arranged shape-memory alloy for hepatic arterial infusion chemotherapy. *Cardiovasc Intervent Radiol* 2010; 33: 1153–1158.
16. Tavallaei MA, Gelman D, Lavdas MK, et al. Design, development and evaluation of a compact telerobotic catheter navigation system. *The Int J Med Rob Comput Assisted Surg* 2016; 12: 442–452.
17. Fu Y, Liu H, Huang W, et al. Steerable catheters in minimally invasive vascular surgery. *Int J Med Rob Comput Assisted Surg* 2009; 5: 381–391.
18. Ali A, Sakes A, Arkenbout EA, et al. Catheter steering in interventional cardiology: mechanical analysis and novel solution. *Proc IMechE, Part H: J Engineering in Medicine* 2019; 233(12): 1207–1218.
19. Jeon SM and Jang GH. Precise steering and unclogging motions of a catheter with a rotary magnetic drill tip actuated by a magnetic navigation system. *IEEE Trans Magn* 2012; 48: 4062–4065.
20. Gosselin FP, Lalande V and Martel S. Characterization of the deflections of a catheter steered using a magnetic resonance imaging system. *Med Phys* 2011; 38: 4994–5002.
21. Rahmer J, Stehning C and Gleich B. Remote magnetic actuation using a clinical scale system. *PLoS One* 2018; 13: e0193546.
22. Leong F, Garbin N, Natali CD, et al. Magnetic surgical instruments for robotic abdominal surgery. *IEEE Rev Biomed Eng* 2016; 9: 66–78.
23. Simi M, Silvestri M, Cavallotti C, et al. Magnetically activated stereoscopic vision system for laparoendoscopic single-site surgery. *IEEE/ASME Trans Mechatron* 2013; 18: 1140–1151.
24. Ryan P and Diller E. Magnetic actuation for full dexterity microrobotic control using rotating permanent magnets. *IEEE Trans Robot* 2017; 33: 1398–1409.